THE JOURNAL OF BIOLOGICAL CHEMISTRY VOL. 286, NO. 23, pp. 20769–20777, June 10, 2011

Polo-like Kinase1 Is Required for Recruitment of Dynein to Kinetochores during Mitosis*[S]

Received for publication, January 30, 2011, and in revised form, April 14, 2011 Published, JBC Papers in Press, April 20, 2011, DOI 10.1074/jbc.M111.226605

Jason R. Bader[‡], James M. Kasuboski[‡], Michael Winding[‡], Patricia S. Vaughan[‡], Edward H. Hinchcliffe[§], and Kevin T. Vaughan[‡1]

From the [‡]Department of Biological Sciences, University of Notre Dame, Notre Dame, Indiana 46556 and the [§]Hormel Institute, University of Minnesota, Austin, Minnesota 55912

Kinetochore dynein has been implicated in microtubule capture, correcting inappropriate microtubule attachments, chromosome movement, and checkpoint silencing. It remains unclear how dynein coordinates this diverse set of functions. Phosphorylation is responsible for some dynein heterogeneity (Whyte, J., Bader, J. R., Tauhata, S. B., Raycroft, M., Hornick, J., Pfister, K. K., Lane, W. S., Chan, G. K., Hinchcliffe, E. H., Vaughan, P. S., and Vaughan, K. T. (2008) *J. Cell Biol.* 183, 819–834), and phosphorylated and dephosphorylated forms of dynein coexist at prometaphase kinetochores. In this study, we measured the impact of inhibiting polo-like kinase 1 (Plk1) on both dynein populations. Phosphorylated dynein was ablated at kinetochores after inhibiting Plk1 with a small molecule inhibitor (5-Cyano-7-nitro-2-(benzothiazolo-*N*-oxide)-carboxamide) or chemical genetic approaches. The total complement of kinetochore dynein was also reduced but not eliminated, reflecting the presence of some dephosphorylated dynein after Plk1 inhibition. Although Plk1 inhibition had a profound effect on dynein, kinetochore populations of dynactin, spindly, and *zw10* were not reduced. Plk1-independent dynein was reduced after p150^{Glued} depletion, consistent with the binding of dephosphorylated dynein to dynactin. Plk1 phosphorylated dynein intermediate chains at Thr-89 *in vitro* and generated the phospho-Thr-89 phosphoepitope on recombinant dynein intermediate chains. Finally, inhibition of Plk1 induced defects in microtubule capture and persistent microtubule attachment, suggesting a role for phosphorylated dynein in these functions during prometaphase. These findings suggest that Plk1 is a dynein kinase required for recruitment of phosphorylated dynein to kinetochores.

Cytoplasmic dynein plays important roles at spindle poles, the cell cortex, and kinetochores during mitosis. The mechanisms that allow dynein to associate specifically with each site remain unknown. One possibility is suggested by the identification of a novel mitotic phosphorylation site in the dynein intermediate chains (ICs)[2] (1). This phosphorylated form of dynein (phospho-Thr-89, pT89) is specific for kinetochores from nuclear envelope breakdown (NEB) to metaphase. Previous work suggests that pT89 dynein is recruited to kinetochores through a direct interaction with *zw10* but undergoes dephosphorylation in response to bioriented microtubule attachment and chromosome alignment. This dephosphorylation of dynein shifts binding to dynactin and stimulates poleward transport of checkpoint proteins; a transition required for the silencing of the spindle assembly checkpoint at metaphase. Defects in this process induce metaphase arrest/delay.

One prediction of this model is that dynein could interact with multiple proteins at kinetochores, depending on the degree of microtubule attachment, microtubule occupancy, and chromosome alignment. Consistent with this scenario, several mitotic proteins have been implicated in interacting with or anchoring kinetochore dynein, including dynactin (2), *zw10* (1, 3), spindly (4, 5), LIS-1 (6), nudE/EL (7–9), and nudC (10). Some of these proteins are likely to affect dynein regulation (11) or motility (1). The contribution of remaining proteins is under investigation. *Zw10* emerges as a central player in dynein recruitment and has been shown to interact with dynactin (12), spindly (4, 5), and nudE/EL (13). The identification of a direct interaction between phosphorylated dynein (pT89) and *zw10* (1) provides additional support for *zw10* and the *rod-zw10-zwilch* complex in dynein recruitment.

Given the complexity of the dynein motor and the multiple roles for dynein during mitosis, new approaches that deplete kinetochore dynein specifically without affecting dynein-associated proteins would improve analysis of dynein function. In this study, we used inhibition of dynein phosphorylation as a tool to reduce kinetochore dynein. Inhibition of Plk1 was sufficient to ablate pT89 dynein accumulation at kinetochores and to induce defects in initial microtubule capture and persistent attachment. In contrast, Plk1 inhibition did not reduce levels of *zw10* or other dynein binding proteins. Finally, Plk1 was able to phosphorylate dynein intermediate ICs at Thr-89 and create the pT89 phospho-epitope. Together these studies suggest that Plk1 is a dynein kinase required for recruitment of dynein to kinetochores.

* This work was supported, in whole or in part, by National Institutes of Health Grants GM60560 (to K. T. V.) and GM072754 (E. H. H.). This work was also supported by American Cancer Society Grant RSG 05-117-01 (to K. T. V.).

[S] The on-line version of this article (available at http://www.jbc.org) contains supplemental videos SV1 and SV2.

[1] To whom correspondence should be addressed: Department of Biological Sciences, University of Notre Dame, Notre Dame, IN 46556. Fax: 574-631-7413; E-mail: Vaughan.4@nd.edu.

[2] The abbreviations used are: IC, intermediate chain; pT89, phospho-dynein; NEB, nuclear envelope breakdown; Plk1, polo-like kinase 1; BTO-1, 5-Cyano-7-nitro-2-(benzothiazolo-N-oxide)-carboxamide; NRK, normal rat kidney; AS, analog-sensitive.

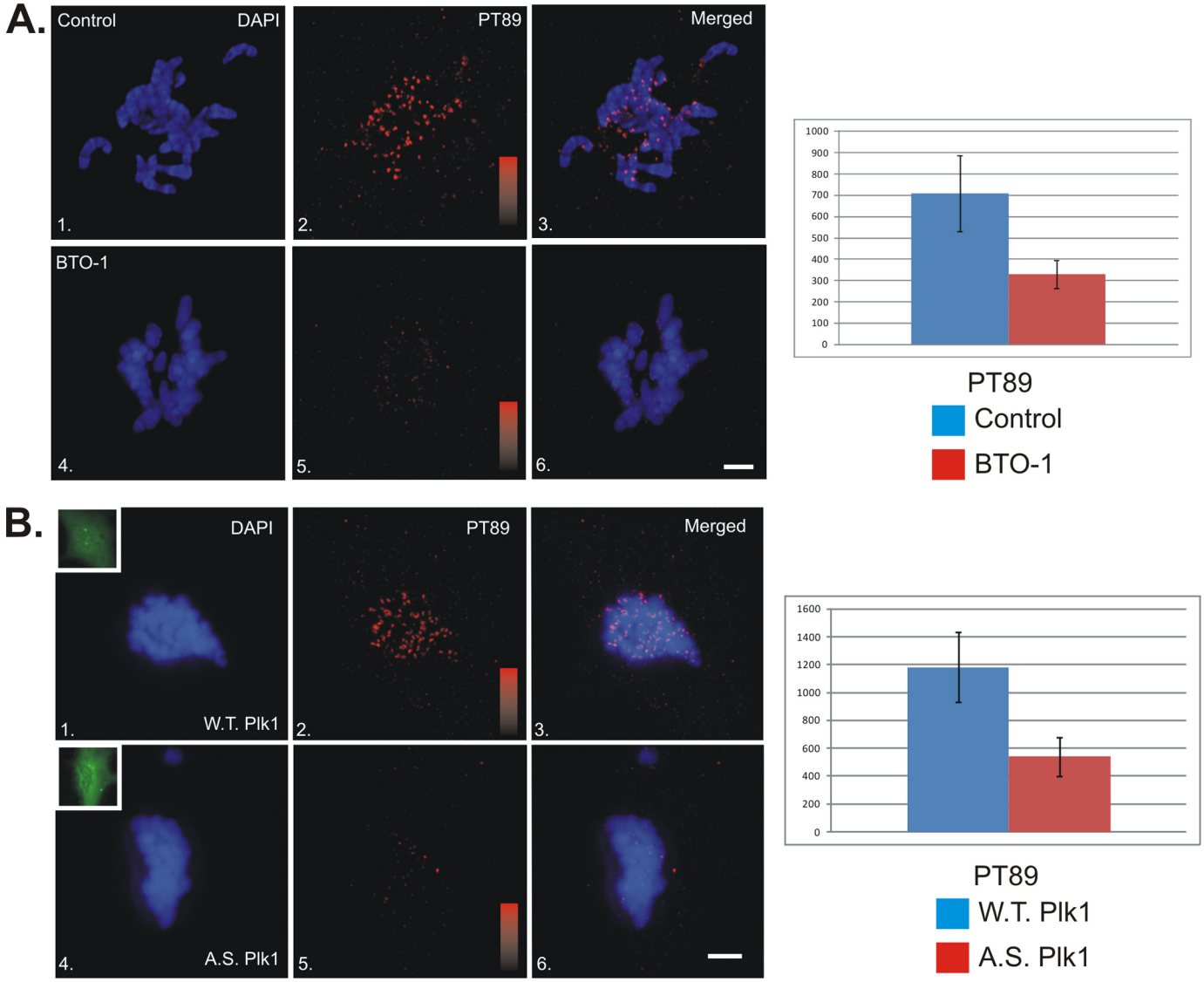

FIGURE 1. **Impact of Plk1 Inhibition of Recruitment of Phospho-dynein to Kinetochores.** *A*, NRK2 cells were treated with vehicle alone (*panels 1–3*) or BTO-1 (*panels 4–6*) and stained for chromatin (*blue*) and pT89 dynein (*red*). BTO-1 treatment resulted in a dramatic reduction in both pT89 dynein and BubR1 at kinetochores during prometaphase. *Intensity scales* = 0–1000 (*panels 2* and *5*). *Scale bar* = 5 μm. Statistical analysis reveals a significant difference for pT89 ($p = 1.28 \times 10^{-16}$). *B*, NRK2 cells were transfected with WT Plk1-GFP (*panels 1–3*) or AS Plk1-GFP (*panels 4–6*), treated with 3MB-PP1, and stained for chromatin (*blue*) and pT89 dynein (*red*). 3MB-PP1 treatment of AS but not WT Plk1 resulted in a dramatic reduction in phospho-dynein at kinetochores during prometaphase. *Intensity scales* = 0–1600 (*panels 2* and *5*). *Scale bar* = 5 μm. *Insets* display expression of GFP constructs (*panels 1* and *4*). Statistical analysis reveals a significant difference for pT89 ($p = 5.49 \times 10^{-29}$).

EXPERIMENTAL PROCEDURES

Chemicals and Reagents—Chemicals were obtained from Sigma-Aldridge (St. Louis, MO) unless indicated otherwise. BTO-1 (EMD, Gibbstown, NJ) was used at a final concentration of 20 μM. Antibodies against the dynein ICs (14), phospho-dynein (pT89 1), p150^{Glued} (15), and *zw10* (16), and tubulin (1) were described previously. Commercially available antibodies were obtained for BubR1 (BD Biosciences) and spindly (Novus, Littleton, CO).

Immunofluorescence Microscopy of Cells—NRK2 and HeLa cells were maintained as described (1). Cell growth on glass coverslips was prepared by MeOH fixation and stained with antibodies against cytoplasmic dynein ICs, the p150^{Glued} subunit of dynactin, BubR1, *zw10*, and spindly, as described previously (1). Images were acquired on a Zeiss Axiovert 200MOT operated with Metamorph software (Molecular Devices, Downingtown, PA) and a Roper Coolsnap HQ camera (Roper, Tucson, AZ). Images were collected at room temperature (fixed cell) or 37 °C (live cell) using a 63× (1.4 numerical aperture) objective. Data were collected as z-series and subjected to digital deconvolution in Metamorph. Because of the image complexity, maximum projections are presented in figures. Using matched illumination, exposure times, and antibody conditions, raw image intensities were used to determine the intensity scales for each experiment. These raw data were maintained through image processing in Adobe Photoshop (Adobe, San Jose, CA) and Coreldraw (Corel, Ottawa, Ontario, Canada) and presented in a pseudocolor scale to convey relative image intensities. For live cell imaging studies, time-lapse image sequences were collected on a similar microscope fit with a Roper Cascade 1k camera. Intensity scales are presented in the figure legends.

In Vitro Kinase Assays—A truncated IC-2 recombinant protein was subjected to *in vitro* phosphorylation as described pre-

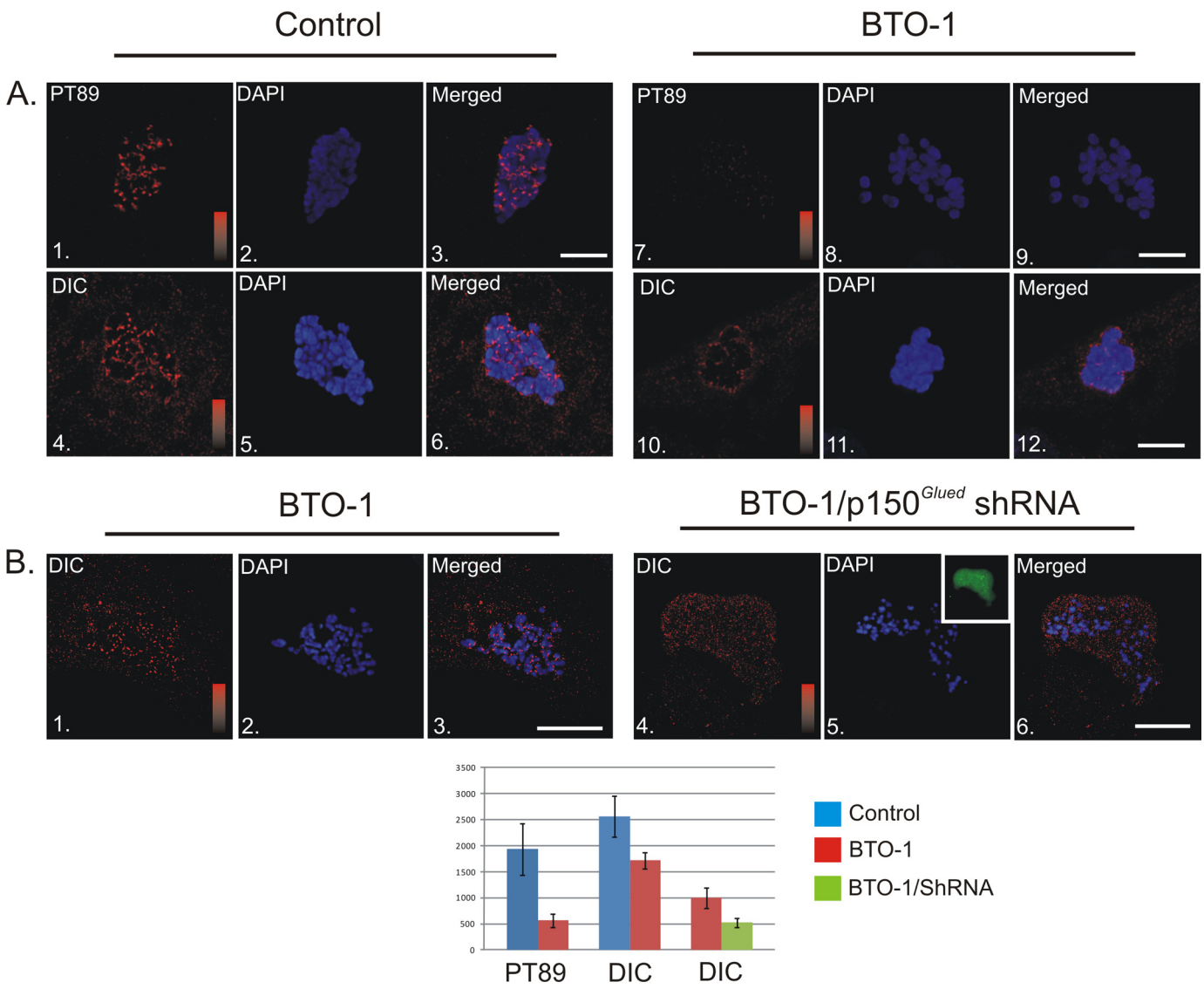

FIGURE 2. **Plk1-dependent and Independent Populations of Dynein at Kinetochores.** *A*, NRK2 cells treated with vehicle control (*panels 1–6*) or BTO-1 (*panels 7–12*) were stained for phosphorylated dynein (*PT89*) or total dynein (*red*) and chromatin (*blue*). Both PT89 dynein and total dynein were reduced significantly at kinetochores after Plk1 inhibition ($p = 5.16 \times 10^{-20}$ for pT89, $p = 5.86 \times 10^{-10}$ for total dynein). However, some total dynein staining remained after BTO-1 treatment. *Intensity scales* = 0–2500 (*panels 1* and *7*) and 0–3000 for total dynein (*panels 4* and *10*). *Scale bar* = 5 μm. *B*, control NRK2 cells and NRK2 cells expressing shRNA plasmid against p150^{Glued} were both treated with BTO-1 and stained for total dynein (*red*) and chromatin (*blue*). Although control cells retain some total dynein after BTO-1 treatment (*panels 1–3*), dynein levels are reduced ($p = 2.26 \times 10^{-6}$) to background in cells depleted of p150^{Glued} and treated with BTO-1 (*panels 4–6*). *Intensity scales* = 0–1500 (*panels 1* and *4*). *Scale bar* = 5 μm.

viously (1), using purified Plk1 (Cell Signaling Technology, Danvers, MA or Cedarlane, Inc., Burlington, NC) and subjected to autoradiography.

Analog-sensitive Plk1 Constructs—Wild-type and analog-sensitive Plk1 constructs (17) were transfected by nucleoporation as described previously (1). Transfected cells were treated with 3MB-PP1 (17).

Chilling/Rewarming Assays—Time-lapse images of NRK cells were captured using a Leica DM RXA2 microscope (Leica Microsystems, Bannockburn, IL) with a Plan Apo 63×/1.3 numerical aperture/37 °C glycerol immersion objective enclosed in a custom-made Plexiglas box maintained at 37 °C and a Hamamatsu ORCA-ER CCD camera (Hamamatsu Photonics, Hamamatsu, Japan). When the chromosomes were judged to have aligned, either vehicle (dimethyl sulfoxide) or BTO-1 was added to the custom-built imaging chamber (18), and then the chamber was chilled (−20 °C for 5 min followed by 35 min at 4 °C (19). The chamber was rewarmed on the microscope for time-lapse imaging, and a nosepiece diamond scribe was used to mark the cell position. After methanol fixation, cells were stained using anti-tubulin and pT89 antibodies.

Statistical Analysis—Statistical analysis of intensity measurements was performed in Microsoft Excel. *p* values of comparisons between control and experimental measurements were determined with a two-tailed *t* test assuming unequal variance. Confidence levels were chosen at $p < = 0.05$.

RESULTS

Impact of Plk1 Inhibition on Kinetochore Dynein—The sequences surrounding the pT89 mitotic dynein phosphorylation site overlap with consensus sites for proline-directed kinases (*X*-S/T-P-*X*) and a polo-binding domain (*X*-S/T-pS/T-P-*X*).

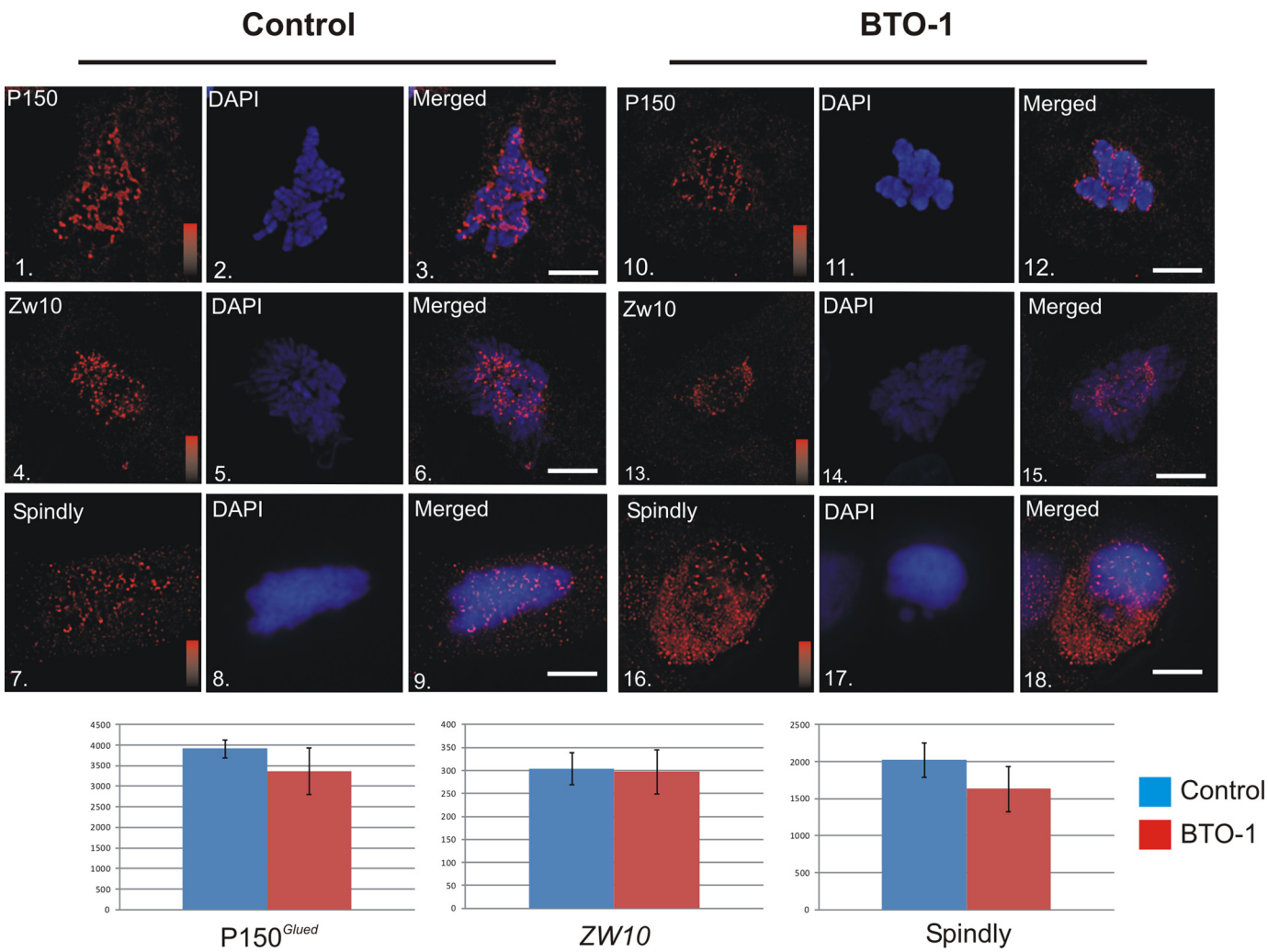

FIGURE 3. **Impact of Plk1 Inhibition on Dynein-associated Proteins.** HeLa cells treated with vehicle control (*panels 1–9*) or BTO-1 (*panels 10–18*) were stained for chromatin (*blue*) and p150^{Glued} (*panels 1–3* and *10–12* (*red*)), *Zw10* (*panels 4–6* and *13–15* (*red*)), or spindly (*panels 7–9* and *16–18* (*red*)). None of these proteins were affected significantly by Plk1 inhibition ($p > 0.05$ for all three). *Intensity scales* = 0–4095 (*panels 1* and *10*), 0–250 (*panels 4* and *13*) or 0–2500 (*panels 7* and *16*). *Scale bar* = 5 μm.

The latter is thought to represent a binding domain for polo-like kinases (20). To test if Plk1 activity plays a role in generating pT89 at kinetochores, we treated NRK2 cells with the small molecule inhibitor BTO-1 (21). This inhibitor has been used to study Plk1 activities at other stages of mitosis (21). Because the levels of pT89 dynein change as chromosomes begin to align at the metaphase plate (1), we measured the impact of BTO-1 treatment early in prometaphase. This allows a comparison of kinetochore dynein levels across the entire complement of chromosomes (1). BTO-1 treatment reduced the levels of pT89 dynein at kinetochores significantly and also reduced the cytoplasmic pool, which is detected normally (Fig. 1*A*). The latter suggests that BTO-1 treatment reduces phosphorylation of dynein at pT89, rather than inhibiting the accumulation of pT89 at kinetochores.

Small molecule inhibitors are powerful tools to study candidate kinases, especially kinases such as Plk1 that are essential and required for multiple stages of mitosis. However, the absolute specificity of some inhibitors is not understood completely. To complement studies with BTO-1, we used analog-sensitive constructs (AS-Plk1) together with nucleotide analogs (3MB-PP1) to inhibit Plk1 (17). The strength of this approach is the specificity of the drugs for the nucleotide binding pocket of mutated Plk1 constructs. In contrast to cells expressing WT-Plk1, cells expressing AS-Plk1 and treated with 3MB-PP1 displayed a marked reduction in pT89 staining (Fig. 1*B*) comparable with BTO-1 treatment alone (*A*). The loss of a cytoplasmic pool of pT89 staining also matched BTO-1 treatment, consistent with a reduction in phosphorylation rather than a reduction in recruitment alone. The similarities in staining for pT89 between BTO-1 and expression of AS-Plk1 constructs suggests that Plk1 is required for recruitment of pT89 dynein to kinetochores during prometaphase.

Multiple Populations of Dynein at Kinetochores—BTO-1 treatment reduced pT89 at kinetochores. However, ongoing studies suggest that dephosphorylated dynein could also accumulate at kinetochores (1). To test this hypothesis, we measured the impact of reducing phosphorylated dynein on accumulation of total dynein. In comparison to controls, levels of total dynein were also reduced significantly after Plk1 inhibition (Fig. 2*A*). Peak kinetochore intensities were reduced ~30%. Interestingly, however, levels of total dynein were not

ablated completely, suggesting the presence of some dephosphorylated dynein on kinetochores even after Plk1 inhibition.

One feature of dephosphorylated dynein is direct binding to the dynactin complex (1, 14). To test whether the BTO-1-resistant population of dynein was dependent on dynactin, we used shRNA-driven depletion of $p150^{Glued}$ to reduce the dynactin complex at kinetochores. As indicated above, Plk1 inhibition alone reduced the levels of total dynein at kinetochores but still permitted some accumulation of dynein. Consistent with previous studies demonstrating a role for dynactin in anchoring a subset of kinetochore dynein (2), BTO-1 treatment coupled with dynactin depletion resulted in a comprehensive loss of dynein at kinetochores (Fig. 2*B*). This suggests that the residual accumulation of dynein after Plk1 inhibition represents a dephosphorylated form of dynein bound to dynactin.

Impact of Plk1 Inhibition on Dynein-associated Proteins—BTO-1 treatment appeared to reduce accumulation of pT89 dynein at kinetochores by reducing phosphorylation (Figs. 1 and 2). However, other mechanisms could explain the reduction, including loss of candidate dynein-associated proteins. To test this possibility, we performed an immunofluorescence microscopy analysis on BTO-1 treated cells and measured levels of dynactin, spindly, and *zw10*. BTO-1 treatment did not have a significant impact on the accumulations of $p150^{Glued}$ (dynactin), spindly, or *zw10* at kinetochores (Fig. 3). Because these represent the core dynein-binding proteins at kinetochores, these results suggest that BTO-1 treatment does not disrupt the overall structure of the dynein-binding platform at kinetochores but rather affects the ability of this platform to recruit dynein.

In Vitro Phosphorylation of Dynein by Plk1—We also considered the possibility that Plk1 inhibition affected dynein recruitment without impacting the phosphorylation of dynein itself. To test whether Plk1 could phosphorylate the dynein ICs directly, we used *in vitro* kinase reactions with recombinant ICs (Fig. 4). The ICs displayed phosphorylation by Plk1 *in vitro*, and this was demonstrated using Plk1 from two different commercial sources (Fig. 4*A*). Phosphorylation was reduced in reactions with the T89A mutant (Fig. 4*A*), and quantification revealed a significant reduction in ^{32}P-incorporation (*B*). These experiments suggest that Plk1 can phosphorylate the dynein ICs *in vitro*, and that *in vitro* phosphorylation is specific for Thr-89.

A phospho-sensitive antibody against the pT89 epitope has been used to monitor dynein phosphorylation *in vivo* and *in vitro* (1). The pT89 antibody does not detect dephosphorylated dynein by Western blot analysis or by IFM analysis. Western blot analysis of recombinant ICs after *in vitro* Plk1 phosphorylation reveals detection of wild-type but not T89A mutant ICs (Fig. 4*C*). This reflects the generation of the pT89 phospho-epitope by Plk1 *in vitro*. Together, these studies suggest that Plk1 can phosphorylate the dynein ICs directly and create a phosphorylated form of dynein analogous to that detected in native samples. The *in vitro* phosphorylation and generation of the pT89 phospho-epitope by Plk1 lends further support to a role for Plk1 in phosphorylating mitotic dynein.

Impact of Dynein Depletion on Prometaphase—Previous studies on kinetochore dynein function have either inhibited dynein globally (22) or disrupted dynein binding proteins (2–7, 23). One benefit of identifying the kinase responsible for kinetochore dynein phosphorylation is the ability to block dynein recruitment without affecting other dynein-binding proteins. To assess the impact of reduced kinetochore dynein on prometaphase progression, we measured errors in kinetochore activity after BTO-1 treatment using live cell imaging. Because Plk1 is required for prophase functions, including spindle pole separation, we added BTO-1 to cells approaching NEB and performed time-lapse imaging (Fig. 5). In contrast to controls, which progressed from NEB to metaphase within ~16 min, BTO-1-treated cells displayed multiple delays and defects during prometaphase (Fig. 5). The most common error was delayed attachment of kinetochores to the mitotic spindle. In addition, once chromosomes approached the metaphase plate, individual chromosomes lost microtubule attachment transiently. Both of these defects extended the time needed to achieve metaphase alignment, and the time from NEB to metaphase completion increased from ~16 min to ~28 min. This is similar

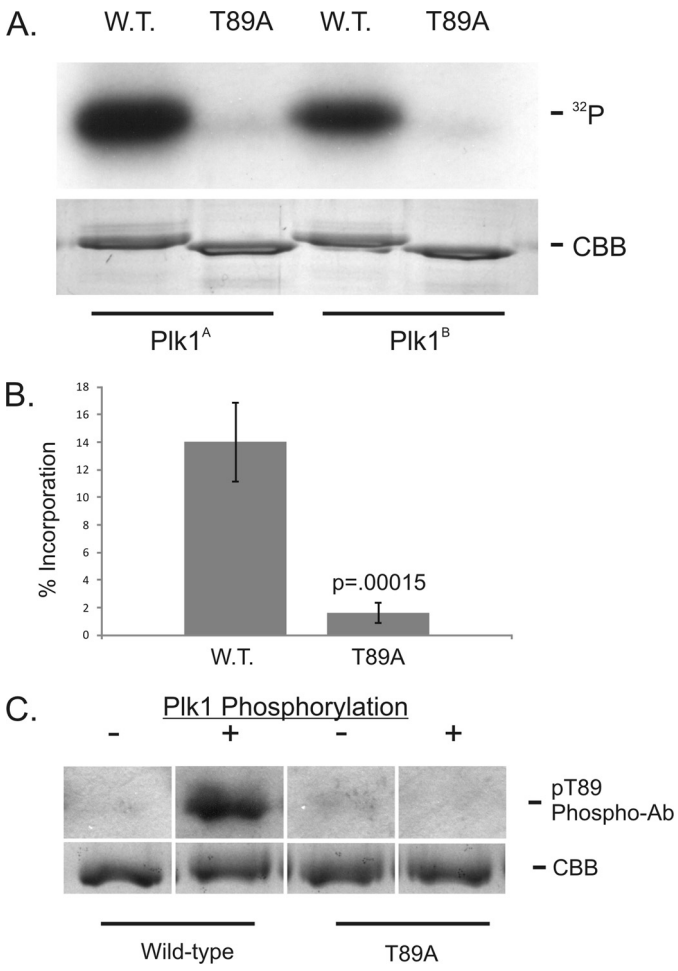

FIGURE 4. ***In Vitro* Phosphorylation of Dynein ICs by Plk1.** *A*, Wild-type and T89A recombinant IC-2C (amino acids 1–284) were subjected to *in vitro* phosphorylation reactions with γ^{32}P-ATP and purified Plk1 (*Plk1^{A}*, Cell Signaling Technology; *Plk1^{B}*, Cedarlane, Inc.). Equal protein loading was confirmed by Coomassie brilliant blue staining of the gel. *B*, Phosphorylation efficiency was measured using the specific activity of γ^{32}P-ATP and IC protein concentration. The *p* value was calculated from four experiments. *C*, wild-type and T89A recombinant IC-2C (amino acids 1–284) were probed by Western blot analysis with the pT89 phospho-antibody before (−) or after (+) Plk1 phosphorylation *in vitro*. Equal loading was confirmed by Coomassie brilliant blue staining of gels run in parallel.

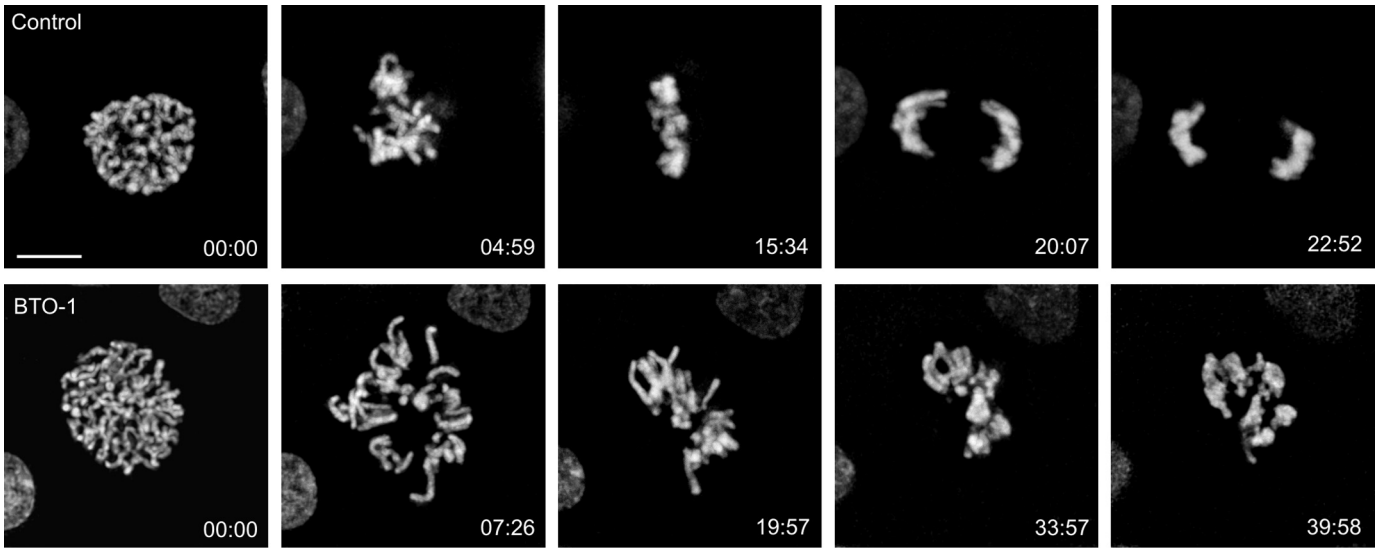

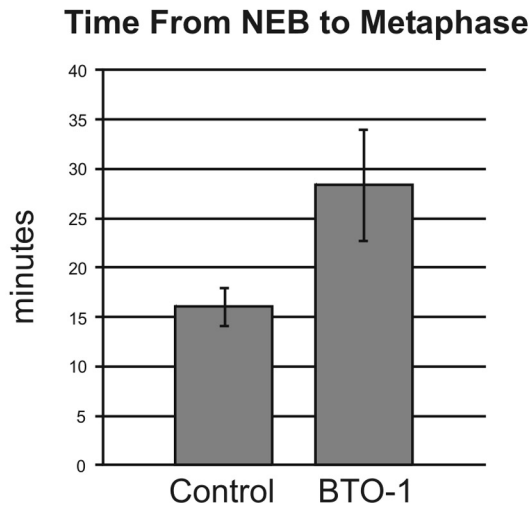

FIGURE 5. **Impact of Plk1 Inhibition on Chromosome Alignment.** NRK2 cells expressing mCherry-H2B were subjected to live-cell imaging after treatment with vehicle control (*Control*) or BTO-1. To overcome the effects of Plk1 inhibition during prophase, cells were treated at NEB and then imaged at 30-s intervals until the metaphase/anaphase transition. Control cells achieved alignment in ~15 min after NEB, whereas treated cells failed to achieve alignment within 30 min after treatment ($p < 0.05$). The most common phenotype is inefficient progression to chromosome alignment (see supplemental videos SV1 and SV2). *Scale bar* = 5 μm.

to phenotypes observed when dynein is disrupted using dominant-negative dynein heavy chain constructs (22) but different from the phenotypes elicited by p50 (dynamitin) expression (*i.e.* metaphase arrest/delay (2)). Because BTO-1 treatment affects dynein without affecting dynactin (Figs. 2 and 3), this suggests that dynein is important for initial events in chromosome attachment and congression, whereas dynactin is required for events closer to the metaphase/anaphase transition. This represents a significant advance over previous studies in which the entire dynein-dynactin complex was perturbed.

Metaphase Kinetochores Retain the Ability to Recruit pT89 Dynein—pT89 dynein accumulation is lost at kinetochores by the time that chromosomes align at the metaphase plate (1). This change has been attributed to the increased activity of PP1γ at metaphase (1) but does not eliminate the possibility that kinetochores lose the ability to recruit dynein by metaphase. We utilized a combination of cell chilling and rewarming at metaphase (19) to test whether metaphase kinetochores continue to recruit pT89 dynein and if this is sensitive to Plk1 inhibition. Mitotic NRK2 cells were screened by differential interference contrast microscopy to identify cells approaching metaphase (Fig. 6). Once chromosome alignment was achieved, cells in custom chambers were shifted to −20 °C (5 min) followed by 4 °C (35 min) to depolymerize spindle microtubules (19). Cells were then warmed to 37 °C for 1–2 min to allow microtubule polymerization and fixed for tubulin and pT89 dynein localization.

Control cells (n = 4) displayed reformation of the mitotic spindle within ~ 2 min. of rewarming, consistent with previous studies (19). The kinetochores of these control cells displayed labeling for pT89 dynein at levels similar to unattached kinetochores (Fig. 6). This indicates that kinetochores retain the ability to recruit pT89 dynein, even after alignment has been achieved. The requirement for Plk1 activity was tested by adding BTO-1 to the cells during the chilling step. Despite the reformation of a typical mitotic spindle in BTO-1-treated cells,

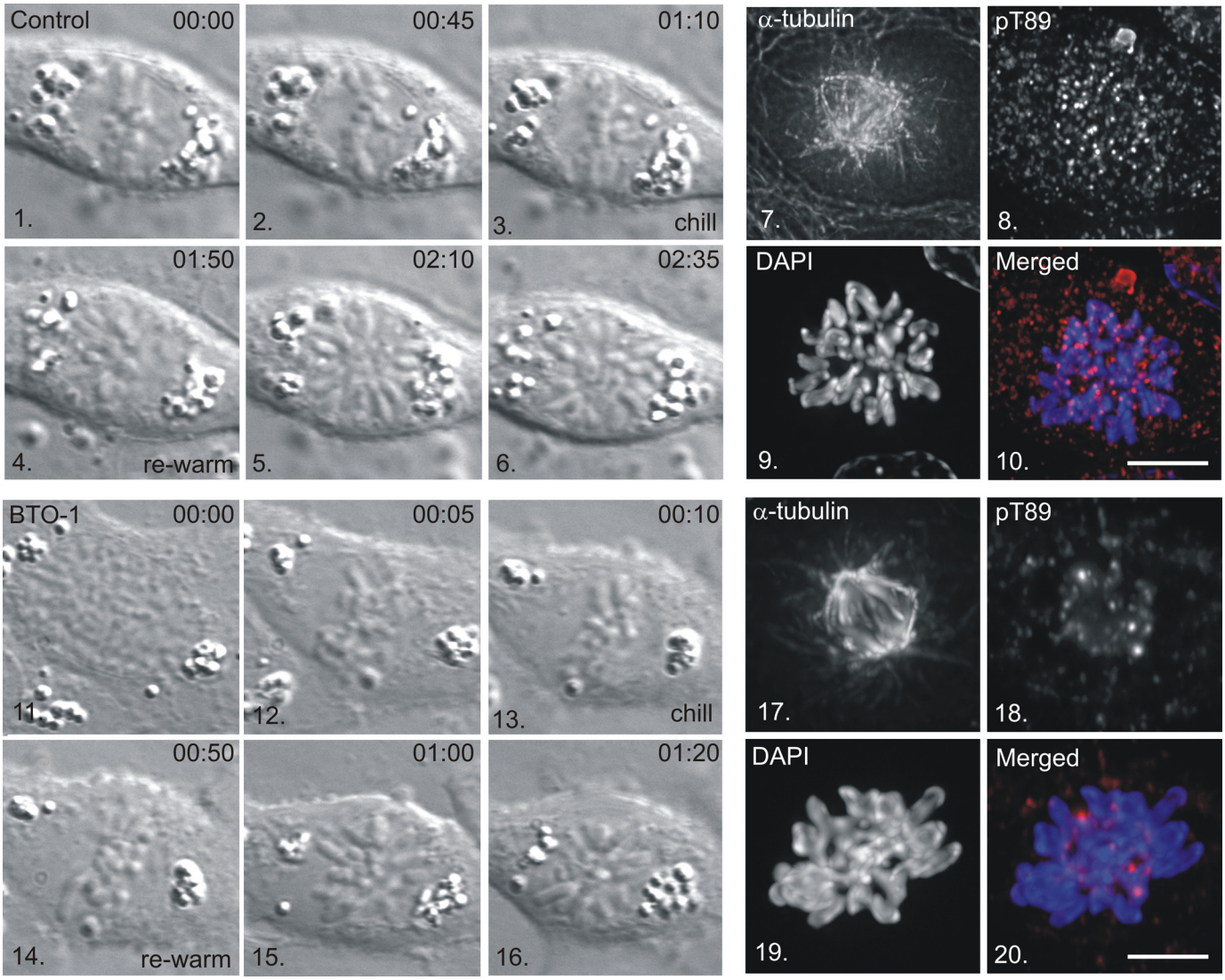

FIGURE 6. **Recruitment of PT89 Dynein to Kinetochores after Metaphase Alignment.** NRK2 cells were monitored by differential interference contrast microscopy until chromosome alignment was achieved (*panels 3* and *13*) and chilled in the presence of a vehicle control (*panels 1–10*) or BTO-1 (*panels 11–20*). Cells were rewarmed (*panels 4–6* and *14–16*), fixed, and stained for α-tubulin (*panels 7* and *17*), pT89 dynein (*panels 8* and *18*), and chromatin (*panels 9* and *19*). Merged images reveal accumulation of pT89 dynein on control (*panel 10*) but not BTO-1-treated (*panel 20*) kinetochores. *Scale bar* = 5 μm.

kinetochores did not accumulate pT89 dynein after rewarming (Fig. 6). Together, these chilling/rewarming experiments reveal that kinetochores retain the ability to recruit dynein throughout prometaphase and into metaphase. This suggests that the changes in pT89 accumulation reflect the dynamics of dynein dephosphorylation and streaming rather than a fundamental change in dynein recruitment activities.

DISCUSSION

These studies provide additional support for the role of phosphorylation in recruitment of cytoplasmic dynein to kinetochores during mitosis and identify a dynein kinase required for this recruitment. Inhibition of Plk1 blocks recruitment of phosphorylated dynein to kinetochores and affects the total pool of dynein at kinetochores significantly. The overall structure of the dynein-binding platform is not affected dramatically. However, Plk1 can phosphorylate the dynein ICs *in vitro* and create the phospho-epitope detected in native samples. Finally, Plk1 inhibition affects kinetochore activities during prometaphase. This is different from previous studies disrupting dynactin that demonstrate an effect at the metaphase/anaphase transition. Together, these studies suggest that Plk1 is a mitotic dynein kinase required for recruitment of dynein to kinetochores (Fig. 7).

Dynein Complexity at Kinetochores—Two major models have emerged to explain the complexity of dynein-binding proteins at kinetochores (24). The first predicts that multiple populations of dynein coexist at kinetochores and are recruited by different mechanisms. The second model predicts that dynein is recruited through a single mechanism but undergoes a series of transitions after recruitment. This study provides insight into these two models.

Inhibition of Plk1 depletes kinetochores of pT89 dynein but does not reduce accumulation of dephosphorylated dynein completely. The identity of this BTO-1-resistant population was revealed after dynactin depletion, which reduced total

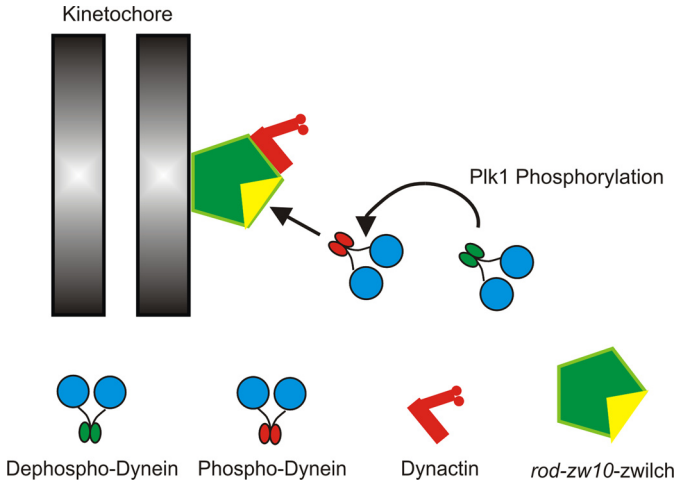

FIGURE 7. **New Model for Recruitment of Dynein to Kinetochores.** Previous work suggested that phosphorylated dynein was recruited to kinetochores through a direct interaction with the *rod-zw10*-zwilch complex (1). However, the requirement for phosphorylation was difficult to test without kinase candidates. This study identifies Plk1 as a mitotic dynein kinase that is required for recruitment of phospho-dynein. This study provides a novel method to separate the contributions of dynactin from those of dynein alone. It also has implications for the application of Plk1 inhibition as an anti-cancer therapy.

dynein levels to background after BTO-1 treatment. Therefore, kinetochores contain a phosphorylated population of dynein (pT89) bound to *zw10* (1) and a dephosphorylated population bound to dynactin (this study). However, it remains unclear whether kinetochore dynactin recruits dephosphorylated dynein independent of the pT89 pathway. Current models suggest that the population of dynein coupled to dynactin is responsible for poleward streaming at metaphase, and that this streaming is required for silencing of the spindle assembly checkpoint in response to chromosome alignment (1). Furthermore, this dephosphorylated dynein is produced from pT89 dynein by PP1γ in response to kinetochore stretch (1). It is possible that the dephosphorylated dynein detected in these studies represents residual dynein that was recruited before complete inhibition of Plk1. This possibility reflects the limitations of Plk1 inhibition, which cannot be initiated until spindle assembly has been accomplished. This scenario is likely, given the kinetics of dynein recruitment to kinetochores once NEB is activated (1). Future experiments will be needed to test this explanation. However, because checkpoint silencing is already linked to a dynein-dynactin complex derived from the pT89 pathway, it remains unclear what the contribution of a dynein-dynactin population independent of the pT89 pathway might be.

Plk1 as a Dynein Kinase—The finding that the dynein ICs are a substrate for Plk1 is intriguing in light of the proposed roles of Plk1 phosphorylation during mitosis. Plk1 is required for spindle pole separation and spindle assembly during prophase (25). During prometaphase, Plk1 also phosphorylates kinetochore proteins, including proteins recognized by the 3F3/2 phospho-antibody (26). Similar to pT89 dynein, which undergoes dephosphorylation in response to chromosome alignment (1), the 3F3/2 phospho-epitope is lost at metaphase (27). Because phosphorylated dynein is not detected by the 3F3/2 antibody by Western blot analysis (data not shown), it appears that 3F3/2 does not detect all Plk1 substrates during mitosis. It is interesting that requirements for dephosphorylation of 3F3/2 phospho-epitopes and dynein at kinetochores are shared.

Analysis of other mitotic dynein kinases has focused on the light intermediate chain subunits (28–30). LIC phosphorylation of the light intermediate chains appears to correlate with entry into mitosis (28) or regulation of membrane binding (29). However, functionally, *cdc2* phosphorylation of LICs is linked to events at the metaphase/anaphase transition rather than early prometaphase (30). Plk1 phosphorylation of the dynein ICs is the first example of regulation that affects initial recruitment to kinetochores (Fig. 7).

Dynein Functions during Prometaphase—Other than studies in which dynein heavy chain constructs were used (22), most previous studies on kinetochore dynein interfered with dynein indirectly through ATP depletion, disrupting dynactin (2), or disrupting other dynein-associated proteins (3–6, 31–33). These approaches lead primarily to problems in checkpoint silencing at metaphase, suggesting that the major role of dynein is poleward streaming (34). Our analysis of dynein dephosphorylation supports this role (1) and demonstrates that loss of streaming leads to metaphase arrest/delay. However, the current study suggests additional roles for dynein during prometaphase that are independent of dynactin. These include microtubule capture, chromosome movement, and efficient progression to metaphase, consistent with previous models (22, 35). As a result, the ability to separate dynein functions from dynein-dynactin functions using Plk1 inhibition advances our understanding of kinetochore dynein activity and the role of dynein accessory proteins.

Acknowledgments—We thank R. B. Vallee (Columbia University) for the contribution of antibodies to Zw10, P. Jallepalli (Memorial Sloan Kettering) for Plk1 constructs, C. Zhang and K. Shokat (University of California at San Francisco) for 3MB-PP1 nucleotide analogs, and members of the Vaughan laboratory for helpful suggestions.

REFERENCES

1. Whyte, J., Bader, J. R., Tauhata, S. B., Raycroft, M., Hornick, J., Pfister, K. K., Lane, W. S., Chan, G. K., Hinchcliffe, E. H., Vaughan, P. S., and Vaughan, K. T. (2008) *J. Cell Biol.* **183,** 819–834
2. Echeverri, C. J., B.M. Paschal, K. T. Vaughan, and R. B. Vallee. (1996) Molecular characterization of the 50-kD subunit of dynactin reveals function for the complex in chromosome alignment and spindle organization during mitosis. *J. Cell Biol.* **132,** 617–633
3. Kops, G. J., Kim, Y., Weaver, B. A., Mao, Y., McLeod, I., Yates, J. R., 3rd, Tagaya, M., and Cleveland, D. W. (2005) *J. Cell Biol.* **169,** 49–60
4. Griffis, E. R., Stuurman, N., and Vale, R. D. (2007) *J. Cell Biol.* **177,** 1005–1015
5. Gassmann, R., Essex, A., Hu, J. S., Maddox, P. S., Motegi, F., Sugimoto, A., O'Rourke, S. M., Bowerman, B., McLeod, I., Yates, J. R., 3rd, Oegema, K., Cheeseman, I. M., and Desai, A. (2008) *Genes Dev.* **22,** 2385–2399
6. Faulkner, N. E., Dujardin, D. L., Tai, C. Y., Vaughan, K. T., O'Connell, C. B., Wang, Y., and Vallee, R. B. (2000) *Nat. Cell Biol.* **2,** 784–791
7. Stehman, S. A., Chen, Y., McKenney, R. J., and Vallee, R. B. (2007) *J. Cell Biol.* **178,** 583–594
8. Liang, Y., Yu, W., Li, Y., Yu, L., Zhang, Q., Wang, F., Yang, Z., Du, J., Huang, Q., Yao, X., and Zhu, X. (2007) *Mol. Biol. Cell* **18,** 2656–2666
9. Vergnolle, M. A., and Taylor, S. S. (2007) *Curr. Biol.* **17,** 1173–1179
10. Zhou, T., Zimmerman, W., Liu, X., and Erikson, R. L. (2006) *Proc. Natl.*

Acad. Sci. U.S.A. **103,** 9039–9044
11. McKenney, R. J., Vershinin, M., Kunwar, A., Vallee, R. B., and Gross, S. P. (2010) *Cell* **141,** 304–314
12. Starr, D. A., Williams, B. C., Hays, T. S., and Goldberg, M. L. (1998) *J. Cell Biol.* **142,** 763–774
13. Starr, D. A., Saffery, R., Li, Z., Simpson, A. E., Choo, K. H., Yen, T. J., and Goldberg, M. L. (2000) *J. Cell Sci.* **113,** 1939–1950
14. Vaughan, P. S., Leszyk, J. D., and Vaughan, K. T. (2001) *J. Biol. Chem.* **276,** 26171–26179
15. Vaughan, K. T., Tynan, S. H., Faulkner, N. E., Echeverri, C. J., and Vallee, R. B. (1999) *J. Cell Sci.* **112,** 1437–1447
16. Varma, D., Dujardin, D. L., Stehman, S. A., and Vallee, R. B. (2006) *J. Cell Biol.* **172,** 655–662
17. Burkard, M. E., Randall, C. L., Larochelle, S., Zhang, C., Shokat, K. M., Fisher, R. P., and Jallepalli, P. V. (2007) *Proc. Natl. Acad. Sci. U.S.A.* **104,** 4383–4388
18. Hornick, J. E., Mader, C. C., Tribble, E. K., Bagne, C. C., Vaughan, K. T., Shaw, S. L., and Hinchcliffe, E. H. (2011) *Curr. Biol.* **21,** 598–605
19. Khodjakov, A., Cole, R. W., Oakley, B. R., and Rieder, C. L. (2000) *Curr. Biol.* **10,** 59–67
20. Park, J. E., Soung, N. K., Johmura, Y., Kang, Y. H., Liao, C., Lee, K. H., Park, C. H., Nicklaus, M. C., and Lee, K. S. (2010) *Cell. Mol. Life Sci.* **67,** 1957–1970
21. Brennan, I. M., Peters, U., Kapoor, T. M., and Straight, A. F. (2007) *PLoS ONE* **2,** e409
22. Varma, D., Monzo, P., Stehman, S. A., and Vallee, R. B. (2008) *J. Cell Biol.* **182,** 1045–1054
23. Gassmann, R., Holland, A. J., Varma, D., Wan, X., Civril, F., Cleveland, D. W., Oegema, K., Salmon, E. D., and Desai, A. (2010) *Genes Dev.* **24,** 957–971
24. Bader, J. R., and Vaughan, K. T. (2010) *Semin. Cell Dev. Biol.* **21,** 269–275
25. Archambault, V., and Glover, D. M. (2009) *Nat. Rev. Mol. Cell Biol.* **10,** 265–275
26. Ahonen, L. J., Kallio, M. J., Daum, J. R., Bolton, M., Manke, I. A., Yaffe, M. B., Stukenberg, P. T., and Gorbsky, G. J. (2005) *Curr. Biol.,* **15,** 1078–1089
27. Gorbsky, G. J., and Ricketts, W. A. (1993) *J. Cell Biol.,* **122,** 1311–1321
28. Dell, K. R., Turck, C. W., and Vale, R. D. (2000) *Traffic,* **1,** 38–44
29. Addinall, S. G., Mayr, P. S., Doyle, S., Sheehan, J. K., Woodman, P. G., and Allan, V. J. (2001) *J. Biol. Chem.,* **276,** 15939–15944
30. Sivaram, M. V., Wadzinski, T. L., Redick, S. D., Manna, T., and Doxsey, S. J. (2009) *EMBO J.,* **28,** 902–914
31. Siller, K. H., Serr, M., Steward, R., Hays, T. S., and Doe, C. Q. (2005) *Mol. Biol. Cell,* **16,** 5127–5140
32. Wojcik, E., Basto, R., Serr, M., Scaerou, F., Karess, R., and Hays, T. (2001) *Nat. Cell Biol.,* **3,** 1001–1007
33. Chan, Y. W., Fava, L. L., Uldschmid, A., Schmitz, M. H., Gerlich, D. W., Nigg, E. A., and Santamaria, A. (2009) *J. Cell Biol.,* **185,** 859–874
34. Howell, B. J., McEwen, B. F., Canman, J. C., Hoffman, D. B., Farrar, E. M., Rieder, C. L., and Salmon, E. D. (2001) *J. Cell Biol.,* **155,** 1159–1172
35. Savoian, M. S., Goldberg, M. L., and Rieder, C. L. (2000) *Nat. Cell Biol.* **2,** 948–952